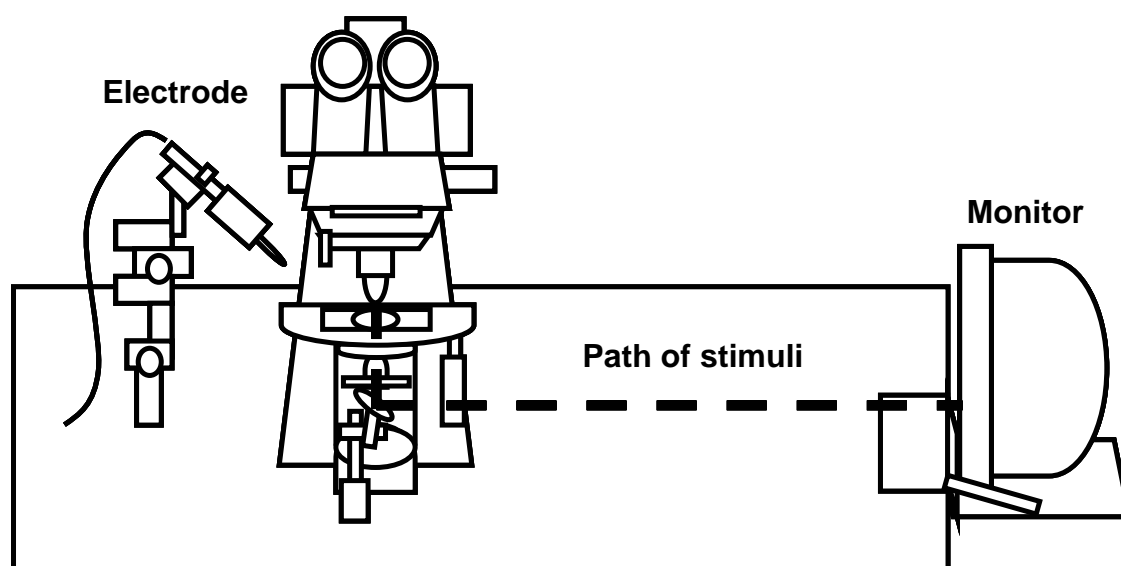
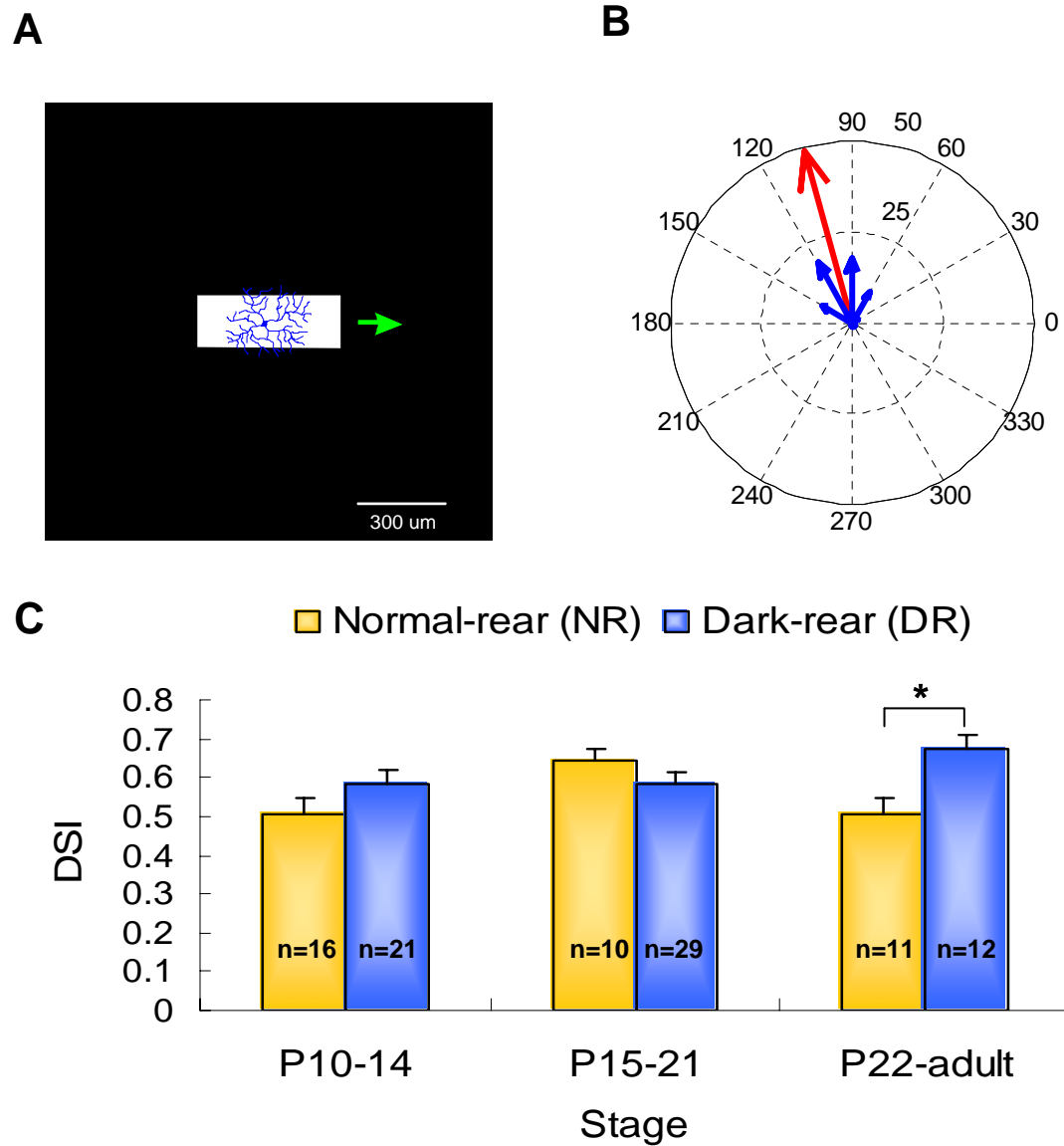


## 6. Figures



**Figure 1. Diagram of the experimental setup for visual stimulus projection and extracellular recording.**

Visual stimuli were displayed on a CRT monitor and reflected upward by a mirror positioned beneath the microscope stage. A 20X microscope objective replaced the condenser was used to focus the stimulus onto the photoreceptor layer of the retina. The dashed line represents the path of stimuli. The activity of the DSGC was recorded with the tungsten-in-glass electrode.



**Figure 2. Direction selectivity can be found in both normal-reared and dark-reared rabbits around eye opening.**

(A) The preferred direction of the DSGCs was determined by a moving bar ( $540 \times 180 \mu\text{m}^2$ ,  $\sim 900 \mu\text{m}/\text{sec} = \sim 5.14 \text{ deg}/\text{sec}$ ) swept across the receptive field in twelve different directions. (B) Blue arrows are vectors pointing in the direction of the moving stimulus and having length equal to the averaged number of spikes recorded

during that stimulus direction. The red arrow indicates vector sum of 12 directions (pointing to the preferred direction). (C) The strength of directional tuning was calculated by direction selective index (DSI;  $\text{mean} \pm \text{s.e.m.}$ ). The DSIs (yellow) of the DSGCs from three different stage groups of P10-14, P15-21, and P22-adult raised under normal light-dark cycle condition were compared to the DSIs (blue) of the DSGCs at the same stage group reared under constant darkness. Number in each column represents the number of the DSGCs studied. \* indicates statistical significance of rearing condition comparison and *P* value is below 0.05.



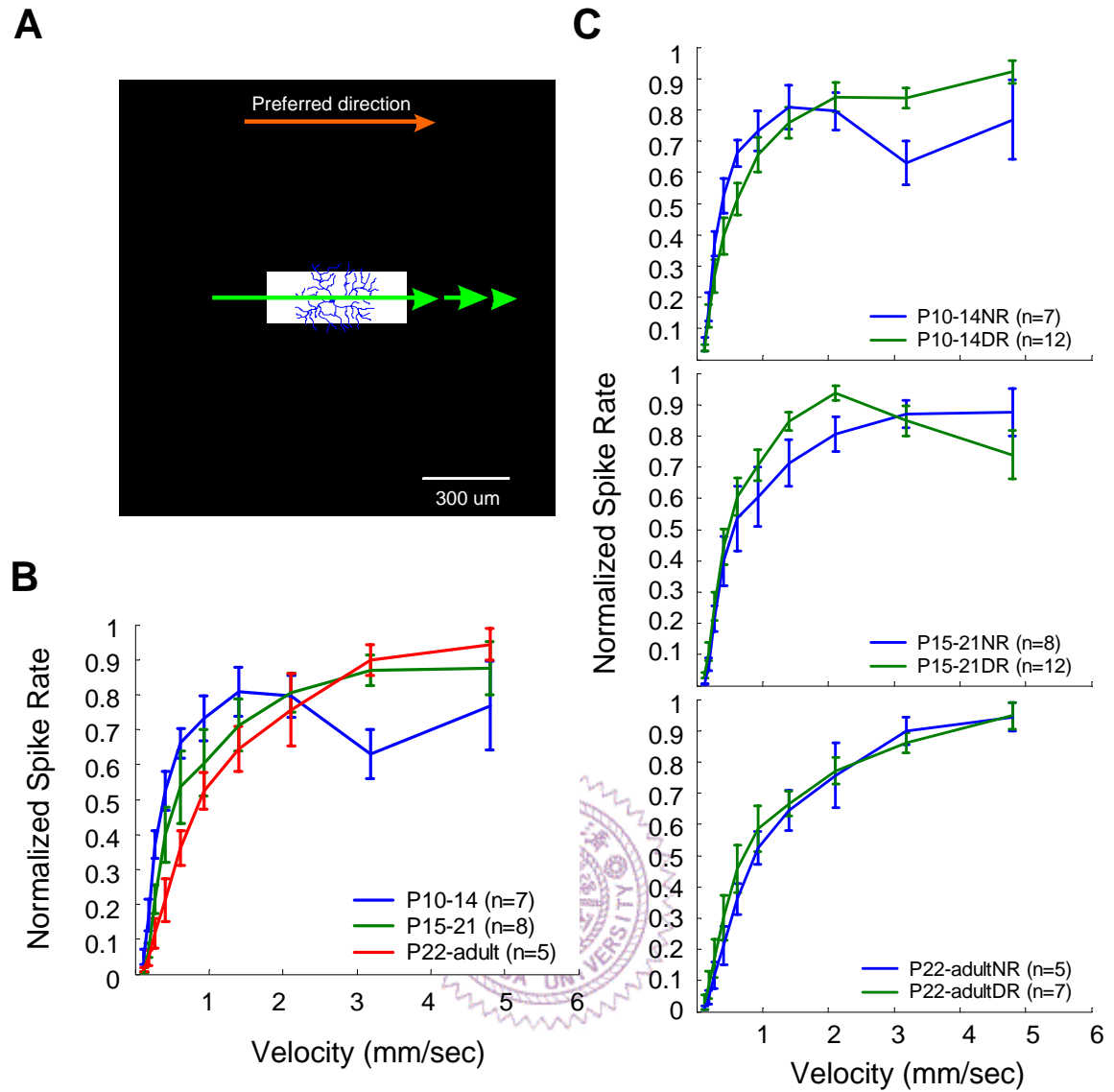


**Figure 3. Velocity tuning of the DSGCs is similar between normal-reared and dark-reared rabbits.**

(A) Velocity tuning was examined by a moving bar ( $540 \times 180 \mu\text{m}^2$ ) swept in the preferred direction with various speeds ( $1 \text{ mm/sec} = 5.71 \text{ deg/sec}$ ). (B) Normalized responses of the DSGCs to various stimulus velocities from three different stage groups of P10-14 (blue), P15-21 (green), and P22-adult (red) raised under normal

light-dark cycle condition (mean  $\pm$  s.e.m.). (C) Normalized responses of the DSGCs to different stimulus velocities from the same stage groups (P10-14, P15-21, and P22-adult) raised under normal light-dark cycle condition (NR, blue) were compared to normalized responses of the DSGCs reared under constant darkness (DR, green). Number in each age group represents the number of the DSGCs studied.



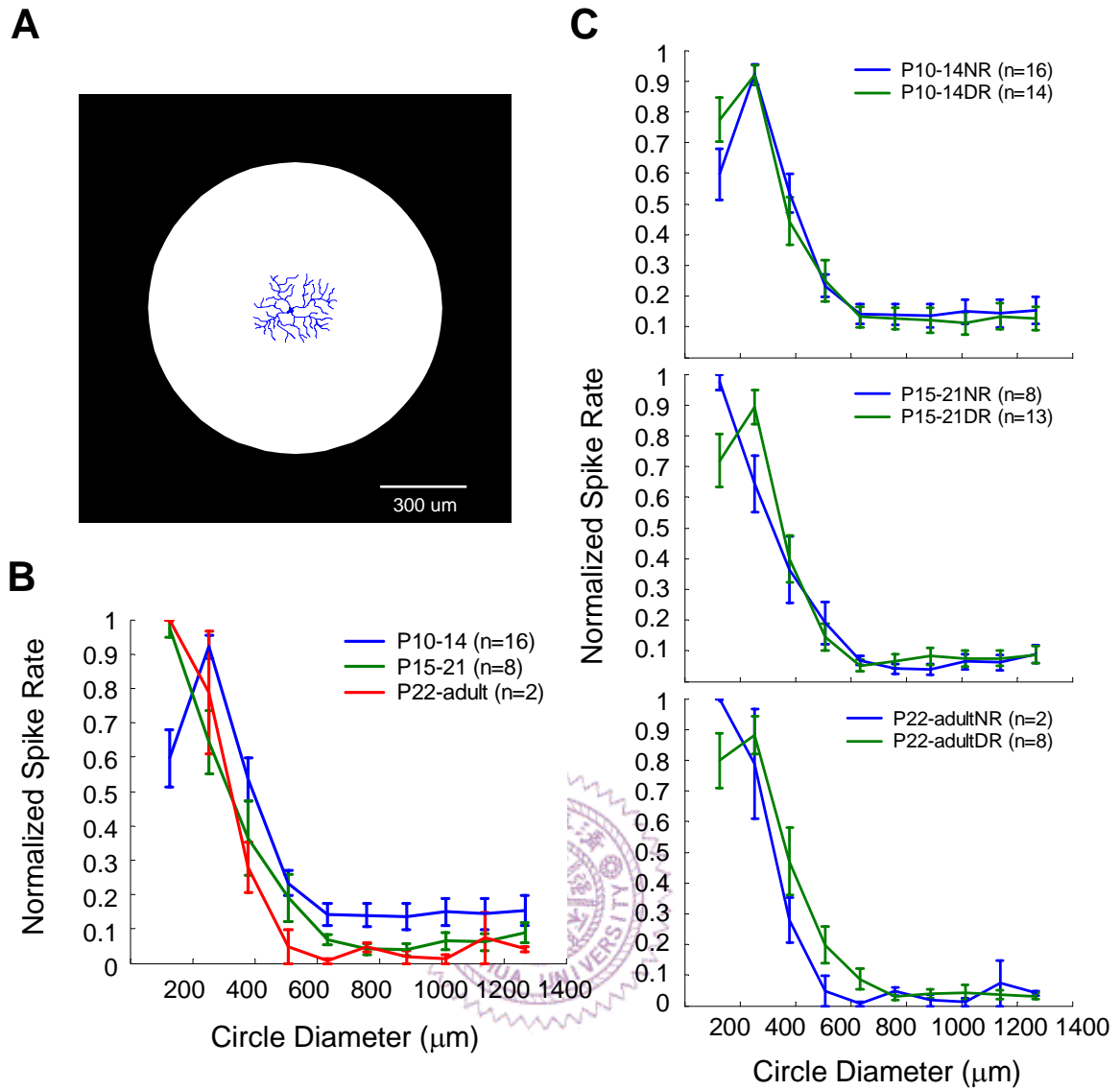


**Figure 4. The DSGCs show classical center-surround receptive field around eye opening in both normal-reared and dark-reared rabbits.**

(A) Center-surround interaction was studied by flashing (167 ms) white circles of different diameters. (B) Normalized responses of the DSGCs to various stimulus sizes from three different stage groups of P10-14 (blue), P15-21 (green), and P22-adult (red) raised under normal light-dark cycle condition (mean  $\pm$  s.e.m.). (C) Normalized

responses of the DSGCs to different stimulus sizes from the same stage groups (P10-14, P15-21, and P22-adult) raised under normal light-dark cycle condition (NR, blue) were compared to normalized responses of the DSGCs reared under constant darkness (DR, green). Number in each stage group represents the number of the DSGCs studied.



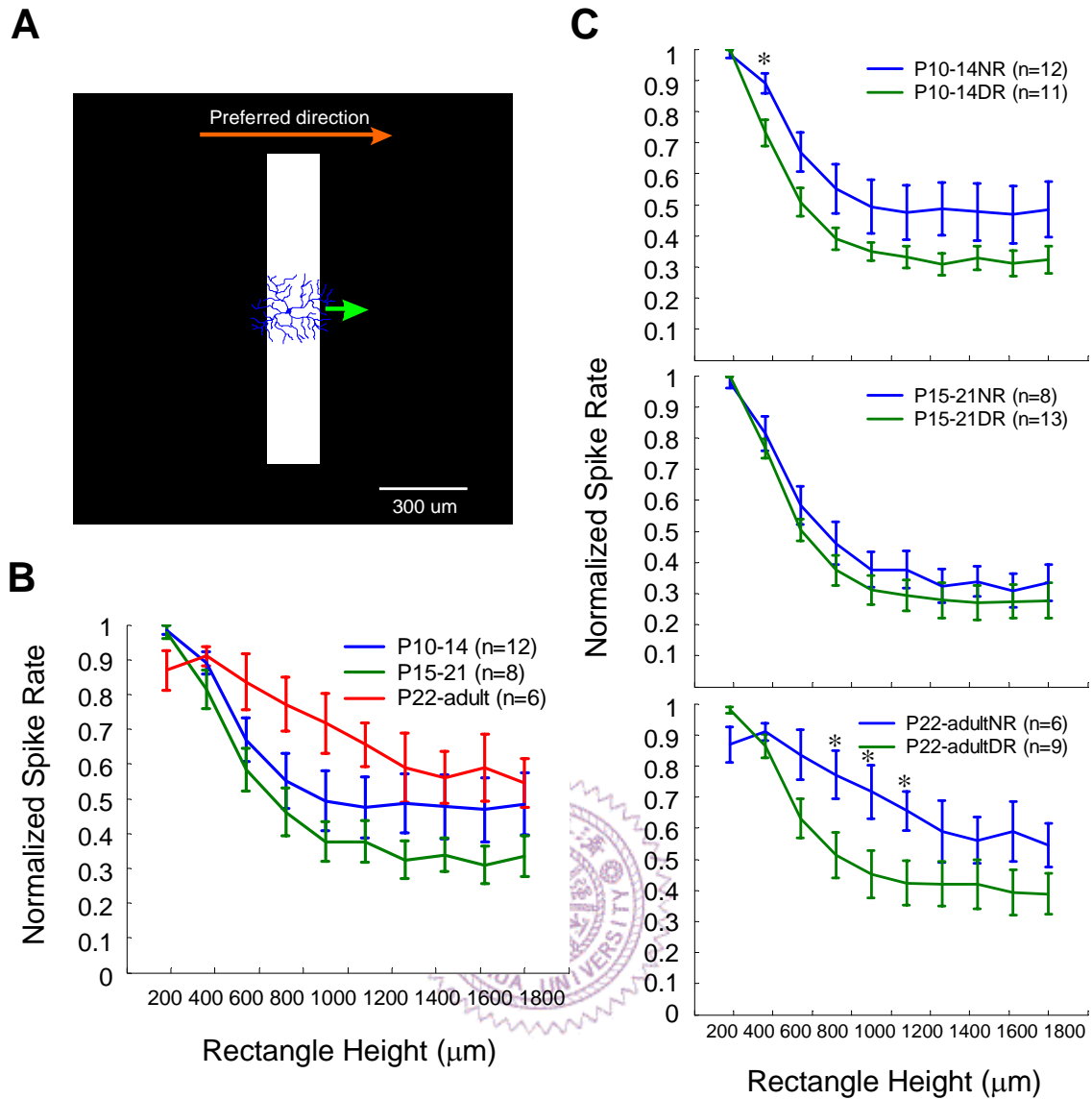


**Figure 5. Surround inhibition induced by preferred direction motion is stronger in dark-reared rabbits.**

(A) Motion surround inhibition induced by preferred direction movement was determined by various sizes of moving rectangles ( $\sim 900 \mu\text{m}/\text{sec} = \sim 5.14 \text{ deg}/\text{sec}$ ) extended perpendicularly to the preferred-null axis swept in the preferred direction. (B) Normalized responses of the DSGCs to various stimulus sizes from three different



stage groups of P10-14 (blue), P15-21 (green), and P22-adult (red) raised under normal light-dark cycle condition (mean  $\pm$  s.e.m.). (C) Normalized responses of the DSGCs to different stimulus sizes from the same stage groups (P10-14, P15-21, and P22-adult) raised under normal light-dark cycle condition (NR, blue) were compared to normalized responses of the DSGCs reared under constant darkness (DR, green). Number in each stage group represents the number of the DSGCs studied. \* indicates statistical significance of rearing condition comparison and *P* value is below 0.05.



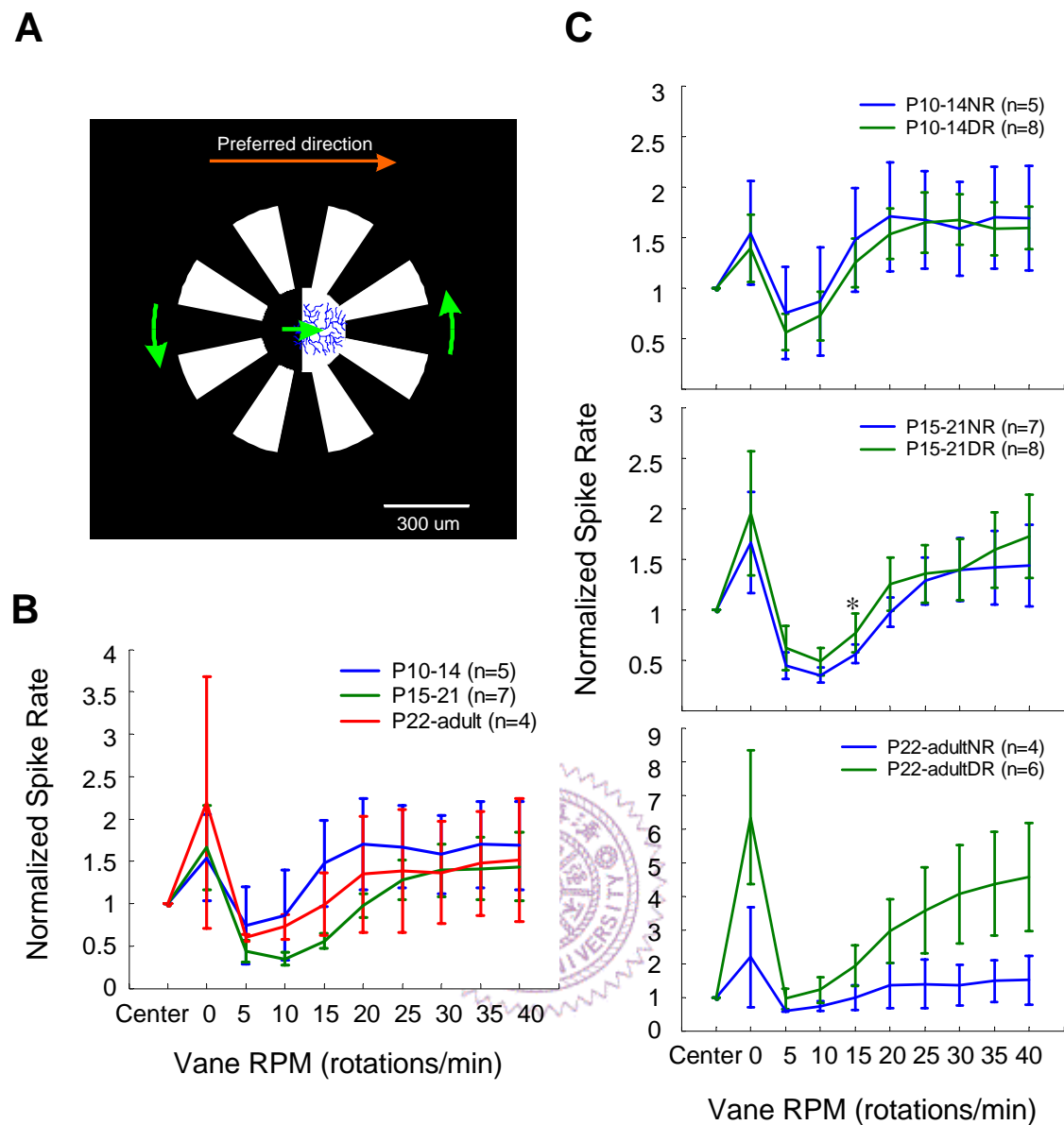


**Figure 6. Motion surround inhibition is less well developed in dark-reared rabbits.**

(A) A square wave grating (1 cycle per receptive field center size) moving in the preferred direction ( $\sim 900 \mu\text{m}/\text{sec} = \sim 5.14 \text{ deg}/\text{sec}$ ) in the receptive field center and a windmill pattern (8 vanes) rotating clockwise in the surround annulus were used to study moving surround inhibition. (B) Normalized responses of the DSGCs to center

alone and different annual stimulus rotations from three different stage groups of P10-14 (blue), P15-21 (green), and P22-adult (red) raised under normal light-dark cycle condition (mean  $\pm$  s.e.m.). (C) Normalized responses of the DSGCs to center alone and different annual stimulus rotations from the same stage groups (P10-14, P15-21, and P22-adult) raised under normal light-dark cycle condition (NR, blue) were compared to normalized responses of the DSGCs reared under constant darkness (DR, green). Number in each stage group represents the number of the DSGCs studied. \* indicates statistical significance of rearing condition comparison and *P* value is below 0.05.



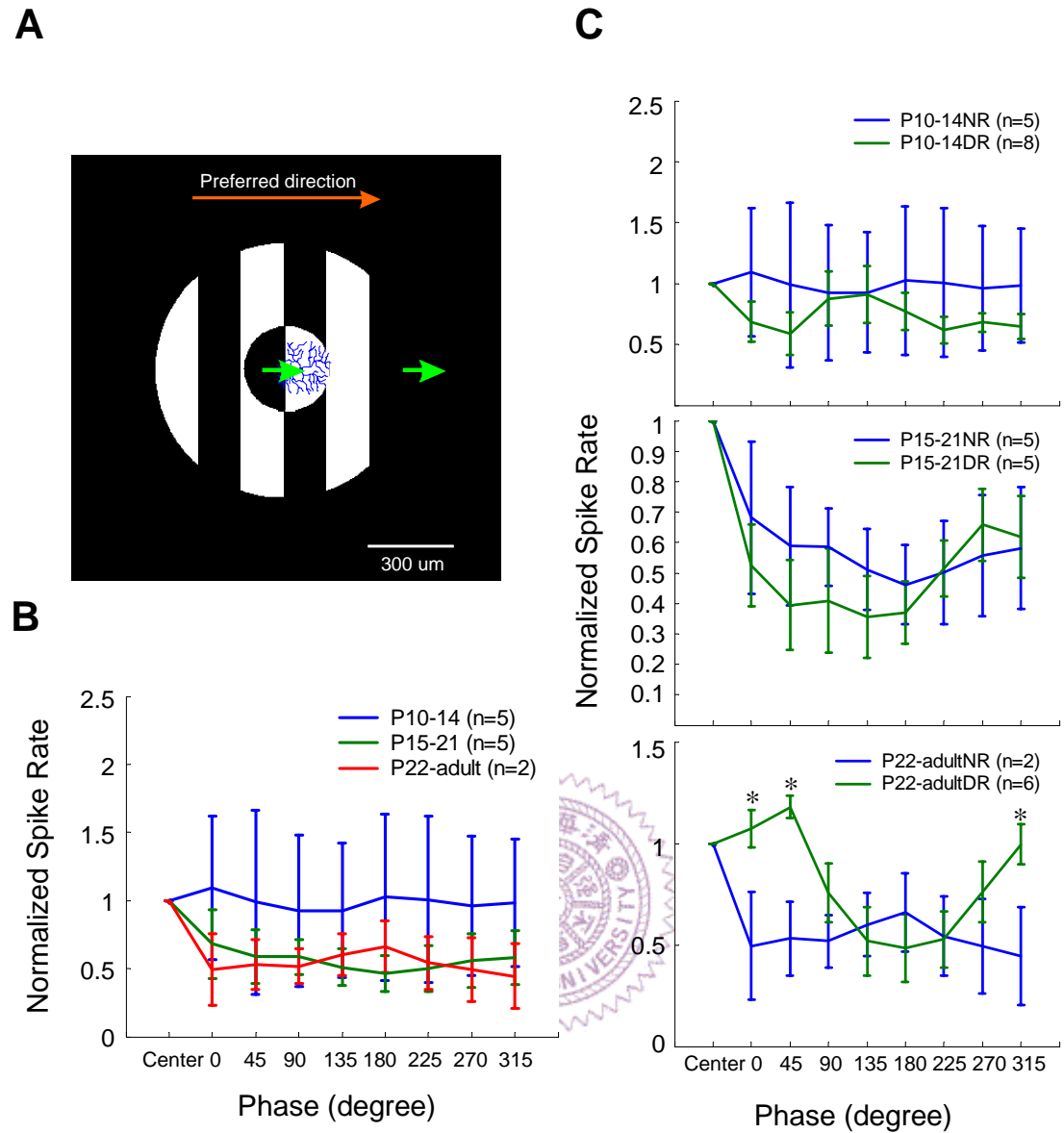


**Figure 7. Contextual tuning is altered in dark-reared rabbits.**

(A) Similar to the stimulus paradigm in Fig. 5A, the surround annulus was replaced by a square wave grating (same spatial and temporal frequency as the center grating) moving in the preferred direction ( $\sim 900 \mu\text{m}/\text{sec} = \sim 5.14 \text{ deg}/\text{sec}$ ). The phase of annulus surround grating was varied to allow center and surround could either in-phase or out-phase to each other. (B) Normalized responses of the DSGCs to center

alone and different stimulus phases from three different stage groups of P10-14 (blue), P15-21 (green), and P22-adult (red) raised under normal light-dark cycle condition (mean  $\pm$  s.e.m.). **(C)** Normalized responses of the DSGCs to center alone and different stimulus phases from the same stage groups (P10-14, P15-21, and P22-adult) raised under normal light-dark cycle condition (NR, blue) were compared to normalized responses of the DSGCs reared under constant darkness (DR, green). Number in each stage group represents the number of the DSGCs studied. \* indicates statistical significance of rearing condition comparison and *P* value is below 0.05.



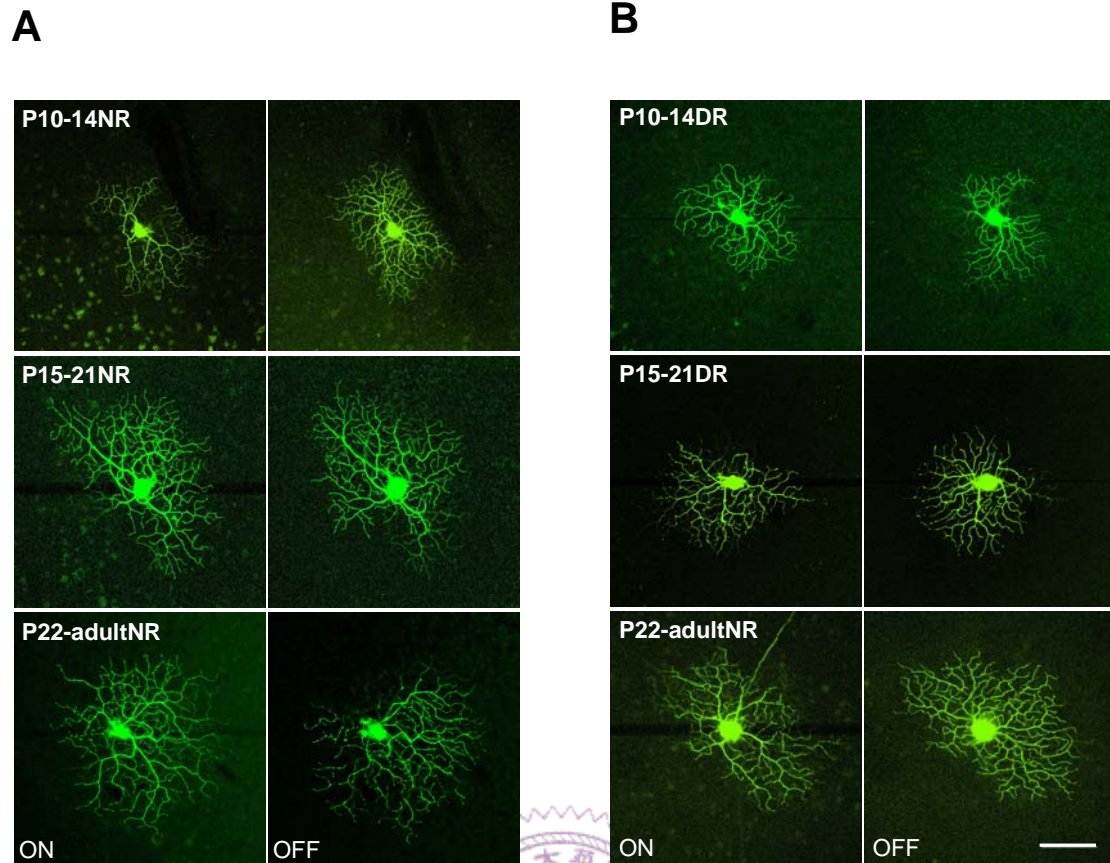


**Figure 8. The DSGCs display characteristic morphological features in both normal-reared and dark-reared rabbits.**

(A) The dendritic morphology of the recorded DSGCs from three different stage groups (P10-14, P15-21, and P22-adult) raised under normal light-dark cycle condition (NR). (B) The dendritic morphology of the recorded DSGCs at the same stage groups reared under constant darkness (DR). ON and OFF dendritic arbors of the DSGCs were separately shown in different columns. Scale bar = 100  $\mu$ m.

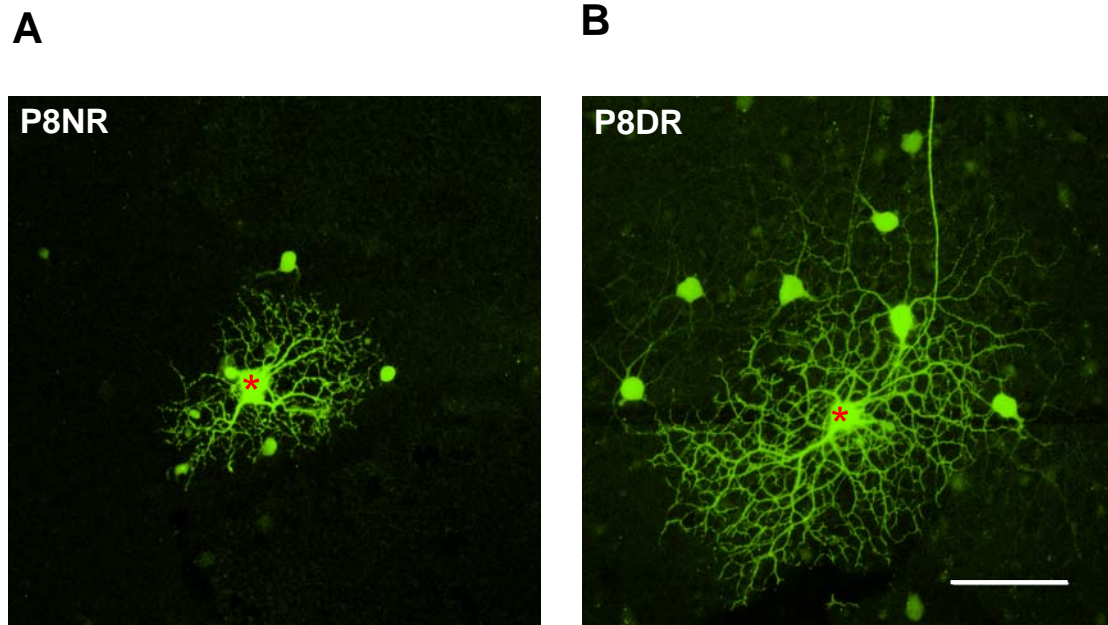


**Figure 9. Tracer coupling patterns of the DSGCs are similar in both normal-reared and dark-reared rabbits at P8.**

(A) The tracer coupling pattern of the recorded DSGC at P8 raised under normal light-dark cycle condition (NR). (B) The tracer coupling pattern of the recorded DSGC at P8 reared under constant darkness (DR). \* indicates the recorded DSGCs.

Scale bar = 100  $\mu$ m.

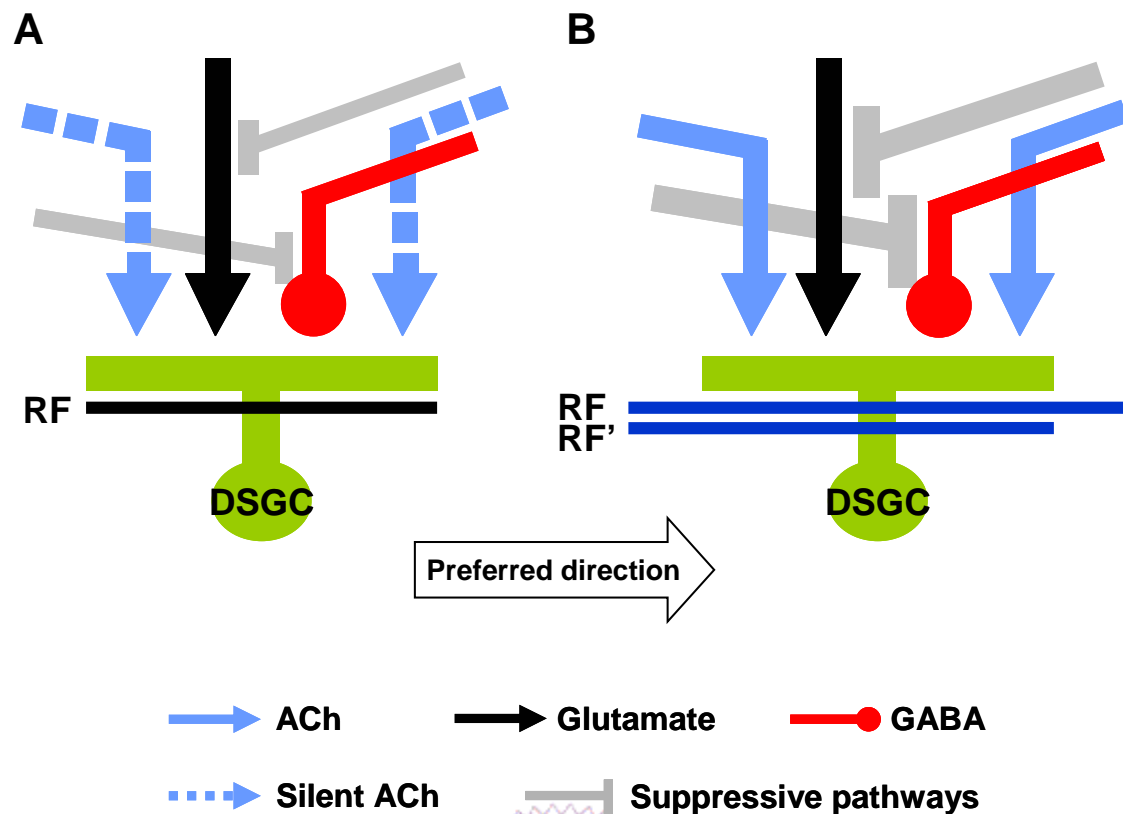


**Figure 10. Schematic diagrams of synaptic circuitry for the DSGCs in the adult and developing rabbits.**

(A) Silent cholinergic pathway and suppressive pathways to the DSGCs in the adult rabbits (modified from Fried et al., 2005). Cholinergic excitatory signal (light blue) to the DSGC is usually blocked. Glutamatergic excitatory input (black) is inhibited by the suppressive pathway (gray) on the null side of the DSGC. GABAergic inhibitory input (red) is inhibited by the suppressive pathway (gray) on the preferred side of the DSGC. The black line beneath dendritic field of the DSGC represents the receptive field of the cell. (B) Active cholinergic pathway and strong suppressive pathways to the DSGCs in the developing rabbits. Cholinergic excitatory signal (light blue) to the



DSGC is not blocked. Glutamatergic excitatory input (black) is strongly inhibited by the suppressive pathway (the thicker gray line) on the null side of the DSGC. GABAergic inhibitory input (red) is vigorously inhibited by the suppressive pathway (the thicker gray line) on the preferred side of the DSGC. The longer dark blue line (closely beneath dendritic field of the DSGC) represents the genuine receptive field of the cell. The shorter dark blue line represents the physiologically-determined receptive field of the cell.



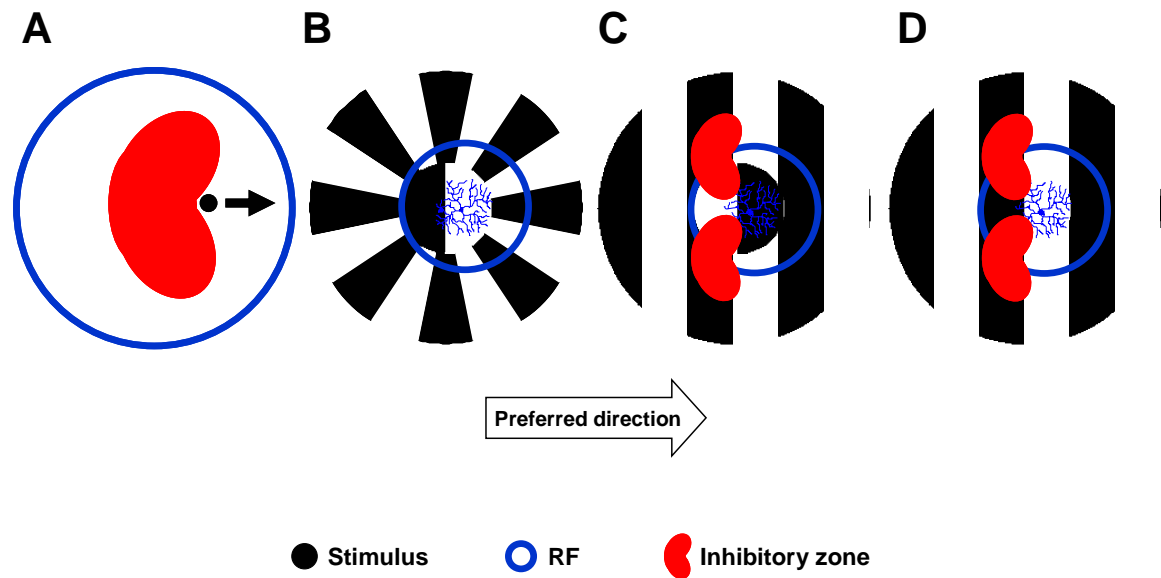


**Figure 11. Inhibitory zones generated by a moving stimulus predict responses of DSGCs in the developing rabbit retinas.**

(A) The stimulus (black dot) moving within the receptive field (blue ring) of the DSGC creates an inhibitory zone (red lobe) falling on the preferred side of the stimulus which suppresses the subsequent stimulation within the zone (modified from Stasheff and Masland, 2002). (B) Motionless windmill within the genuine receptive field (blue ring) of the DSGC does not produce an inhibitory zone. (C) Inhibitory zones (red lobe) of out-of-phase surround grating within the genuine receptive field (blue ring) largely fall on the center grating stimulation. (D) Inhibitory zones (red lobe) of in-phase surround grating within the genuine receptive field (blue ring) slightly fall on the center grating stimulation.